



Analysis of Entropy Generation in Hydromagnetic Micropolar Fluid Flow over an Inclined Nonlinear Permeable Stretching Sheet with Variable Viscosity

Ephesus Olusoji Fatunmbi¹, Sulyman Olakunle Salawu²

¹ Department of Mathematics and Statistics, Federal Polytechnic, Ilaro, Nigeria, E-mail: ephesus.fatunmbi@federalpolyilaro.edu.ng

² Department of Mathematics, Landmark University, Omu-Aran, Nigeria, Email: kunlesalawu@yahoo.com

Received September 06 2019; Revised December 10 2019; Accepted for publication December 10 2019.

Corresponding author: E.O. Fatunmbi (ephesus.fatunmbi@federalpolyilaro.edu.ng)

© 2020 Published by Shahid Chamran University of Ahvaz

& International Research Center for Mathematics & Mechanics of Complex Systems (M&MoCS)

Abstract. A numerical analysis is performed on entropy generation in a radiative and dissipative hydromagnetic micropolar fluid prompted by a nonlinearly stretching sheet with the impact of non-uniform heat source/sink, variable magnetic field, electrical conductivity, and dynamic viscosity. The main equations are computationally solved via shooting techniques in the company with Runge-Kutta algorithms. The impact of the prominent controlling parameters is graphically checked on the velocity, temperature, microrotation, entropy generation, and Bejan number. An excellent relationship exists between the results obtained with related studies previously reported in the literature in the limiting conditions. More so, it is revealed by the findings that the irreversibility due to heat transfer is dominant over viscous dissipation irreversibility as the radiation parameter advances while the trend changes with the Brikman number parameter.

Keywords: Entropy generation; Micropolar fluid; Inclined sheet; Variable viscosity; Stretching sheet.

1. Introduction

The micropolar fluid has gained prominence among other non-Newtonian fluids owing to its special characteristics in modeling and simulating various complex and complicated fluids with rigid, bar-like particles. These fluids consist of microstructure and cannot be effectively explained by the Navier-Stokes model. Such fluids include polymeric fluids, fluid suspensions, animal blood, lubricants, liquid crystals, colloidal fluids and so on [1-2]. The micropolar fluid concept as derived by Eringen [3-4] has to do with the category of fluids which tend to display some microscopic effect resulting in both translation and rotation of the fluid element. In this model, the field of microrotation and macro-velocity are coupled together. The possible applications of such fluids in engineering and industrial operations can be found in the bio-mechanic and chemical engineering, extrusion of polymer, slurry technologies, synovial lubrication, arterial blood flows, knee cap mechanics, a few of many [5-7].

The study of boundary layer flow activated by stretching sheet has since been considered by various researchers from the time it was initially reported by Sakiadis [8]. Subsequently, Crane [9] analytically investigated such a problem on a two-dimensional linearly stretching sheet where the velocity and the distance from the slit vary proportionally to each other. This kind of study is applicable in textile production, extrusion of plastic sheet and metal, ceramic engineering operations, drawing of copper wires, glass blowing, etc. In view of these consequential applications, various scientists and researchers [10-14] have researched this subject considering different parameters, boundary conditions, and geometries. Meanwhile, it has been observed that the stretching of the sheet may not always be linear (see Cortell [15]). To this end, [15-16] studied heat transfer problems on nonlinear sheet with the impact of viscous dissipation and

radiation with constant and prescribed surface temperature conditions on the wall, Alinejad and Samarbakhs [17] numerically investigated such problem with uniform surface temperature while Daniel [18] also reported such subject on nanofluid with convective heat transfer. However, unlike the previous authors who discussed only on Newtonian fluid, [19-21] have examined the situations where the fluid is a non-Newtonian micropolar type over a nonlinearly stretching sheet with various parameters of interest. In these studies, however, magnetic field effects have been ignored in spite of its importance.

The benefits derived from the study of hydromagnetic fluid flow coupled with heat transfer characteristics passing stretching sheets are enormous both in the manufacturing and engineering processes particularly in the metal-working and metallurgical operations for instance, in MHD generators, nuclear reactors geothermal energy extractions, etc. [22]. The magnetic field can be used to heat up, pump, levitate liquid metals and for purifying molten metals from non-metallic inclusions. In view of these crucial applications, Kumar and Srinivas [22] addressed the hydromagnetic fluid flow of non-Newtonian Eyring-Power type with nanofluid passing through an inclined surface being influenced by radiation and Joule heating. Similarly, Waqas *et al.* [23] investigated MHD flow of micropolar fluid induced by a nonlinear stretching sheet with viscous dissipation and Joule heating effects while Shamshuddin and Thumma [24] numerically discussed heat and mass transfer characteristics of a micropolar fluid along an inclined plate in a porous medium under the influence of magnetic field.

The above studies, however, have been carried out with the assumption of constant fluid properties but it has been observed that the fluid physical properties especially the viscosity is dependent on the temperature. It has also been verified that a rise in temperature causes the transport phenomena to escalate due to a decrease in the viscosity across the hydrodynamic boundary layer which could also affect the thermal boundary layer as well as the rate of heat transfer at the surface [19]. Experiments have also revealed that the strength of viscosity is proportional to the temperature in gases while in liquids it is inversely related (see Khan *et al.* [25]). For a realistic solution, therefore, it is crucial to examine the variation of viscosity with temperature in the flow field. In view of various engineering and industrial applications attached to such studies such as in hot rolling, food processing, the process of wire drawing, paper and textile production, [22] discussed the effect of variable viscosity in hydromagnetic Newtonian fluid past a heated sheet. Rahman [26] examined the influence of variable fluid properties with the convective condition at the boundary. Also, researchers such as [27-28] have examined such a study where the viscosity has either direct or inverse relation with the temperature on both Newtonian and non-Newtonian micropolar fluids. Meanwhile, all these were carried out only with the first law of thermodynamics, however, investigations conducted with the second law of thermodynamics which corresponds to entropy generation have been found to be dependable than those conducted using the first law (see Kobo and Makinde [29]).

The study of entropy generation in a system has been a concern to researchers due to the practical applications of such subjects in various areas. In heat transfer problems, entropy generation is a means of measuring the irreversibility that takes place in a system with the use of the second law of thermodynamics [29]. The entropy generation also measures the level of the work destruction that is available in a system, therefore, it becomes germane to figure out the entropy generation rate in a system with a bid to upgrade such a system. Furthermore, research into entropy generation in a system sheds light on the sources by which available energy is destroyed in a system such that it becomes clear that those sources which contribute to entropy can be identified and possibly minimized as to achieve optimal energy needed in a system. Such a concept was initiated by Bejan [30-31] while studying heat transfer and thermal design by the use of the second law of thermodynamics. Also, Makinde [32] in a related work discussed the combined influence of radiative and dissipative hydromagnetic Newtonian fluid with varying viscosity and entropy generation while Salawu *et al.* [33] reported entropy generation analysis of hydromagnetic Powell-Eyring fluid flow having variable conductivity with the influence of chemical reaction in a porous channel. Recently, a numerical approach via Finite difference technique was employed by Alsabery *et al.* [34] to analyze entropy generation with natural convection using nanofluid being influenced by varying temperature distributions. Meanwhile, Afridi *et al.* [35] numerically examined mixed convection entropy generation in MHD Newtonian fluid moving along an inclined sheet. In the light of engineering usefulness derived from studies related to entropy production analysis, various researchers have investigated such studies with different parameters, geometries, wall conditions and various kinds of fluids (see [36-40]). All these researches were however carried out on a linearly stretching sheet without due consideration for nonlinear stretching surfaces which is the focus of this study.

In particular, the current study tends to analyze entropy generation in a hydromagnetic micropolar fluid passing an inclined nonlinear permeable stretching sheet with variable electrical conductivity and temperature-dependent viscosity. A numerical solution is carried out to identify and discuss the impact of different parameters incorporated in the work. Considering the enormous works done on irreversibility analysis on various geometry, attention has not been given to the problem discussed in this work in the literature. Specifically, this study is an extension to the work of [35] with the following under listed uniqueness:

- This work has been conducted with non-Newtonian micropolar fluid as against the Newtonian fluid engaged by those authors.
- It generalizes the work of [35] by considering a nonlinear surface instead of a linear surface of those authors.
- The influence of temperature-dependent viscosity effect which the authors did not consider in spite of its importance.
- The presence of the effect of radiation effect and that of suction/injection in the present work which was neglected by those authors.

- The inclusion of the Joule heating effect as well as that of the heat source/sink effect which was not accounted for in [35].

2. Mathematical Development of the Model

The model investigated in this study consists of the entropy production analysis on a two-dimensional steady flow of an incompressible hydromagnetic micropolar fluid along with a nonlinearly stretching sheet that is inclined at angle φ as illustrated in Fig. 1. The electrical conductivity is dependent on the velocity component u in the x direction (see Eq. 6), the applied magnetic field parallel to y axis is normal to the flow direction and is a function of x as $B = (0, B(x))$ (see Eq. 7) with x being the coordinate along the surface while B_0 is strength of the magnetic while the induced magnetic field is assumed to be negligible. The dynamic viscosity is assumed to be inversely proportional to temperature (see Eq. 9) while the heat source/sink is assumed to be non-uniform (see eq. 8). The sheet stretches with a velocity $u = cx^r$, along x direction where $c > 0$ is a constant and r is the nonlinear stretching parameter. The influences of pressure gradient, electric field and body forces are neglected.

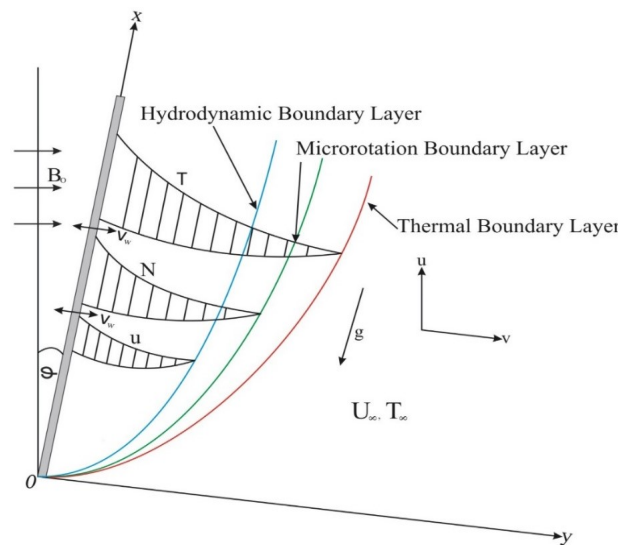


Fig. 1. The Sketch of the Physical Model

In view of the Boussinesq and boundary layer approximations together with the aforementioned assumptions, the modeled equations are stated as ([41-42])

$$u \frac{\partial u}{\partial x} + v \frac{\partial v}{\partial y} = 0. \tag{1}$$

$$u \frac{\partial u}{\partial x} + v \frac{\partial u}{\partial y} = \frac{1}{\rho_\infty} \frac{\partial}{\partial y} \left(\mu \frac{\partial u}{\partial y} \right) + \frac{\mu_r}{\rho_\infty} \frac{\partial^2 u}{\partial y^2} + \frac{\mu_r}{\rho_\infty} \frac{\partial \omega}{\partial y} + g_x \beta_T (T - T_\infty) \cos \varphi - \frac{\sigma_0 (B(x))^2}{\rho_\infty} u, \tag{2}$$

$$u \frac{\partial \omega}{\partial x} + v \frac{\partial \omega}{\partial y} = \frac{\gamma}{\rho_\infty j} \frac{\partial^2 \omega}{\partial y^2} - \frac{\mu_r}{\rho_\infty j} \left(2\omega + \frac{\partial u}{\partial y} \right) \tag{3}$$

$$u \frac{\partial T}{\partial x} + v \frac{\partial T}{\partial y} = \frac{k}{\rho_\infty c_p} \left(1 + \frac{16\sigma^* T_\infty^3}{3k^* k} \right) \frac{\partial^2 T}{\partial y^2} + \frac{\mu + \mu_r}{\rho_\infty c_p} \left(\frac{\partial u}{\partial y} \right)^2 + \frac{\sigma_0 (B(x))^2}{\rho_\infty c_p} u^2 + \frac{q'''}{\rho_\infty c_p} \tag{4}$$

The relevant boundary conditions for this model are as follows:

$$y = 0 : u = u_w = cx^r, v = v_w, \omega = -h \frac{\partial u}{\partial y}, T = T_w = (Ax^n + T_\infty), \tag{5}$$

$$y \rightarrow \infty : u \rightarrow 0, \omega \rightarrow 0, T \rightarrow T_\infty.$$

The wall temperature parameter is indicated by n , while the suction/injection term is denoted by v_w with $v_w = V_0 x^{\frac{(r-1)}{2}}$ [43-44] where V_0 is a constant and h is a boundary parameter having characteristics $0 \leq h \leq 1$. The electric

conductivity is assumed to be (see Helmy [45]):

$$\sigma_0' = \sigma_0 \mu \tag{6}$$

also, the magnetic field is a function of x given as ([6, 42]).

$$B(x) = \frac{B_0}{\sqrt{x}} \tag{7}$$

where σ_0 and B_0 are constants. Following [46], the non-uniform heat source/sink q''' written in eq. (4) is expressed as:

$$q''' = \frac{k u_w}{x^r \nu} [H^* (T_w - T_\infty) f' + J^* (T - T_\infty)] \tag{8}$$

with $H^* = b x^{r-1}$ and $J^* = b^* x^{r-1}$ being the space and heat dependent source/sink respectively. When $H^* > 0$ and $J^* > 0$ then heat is generated whereas heat is absorbed when $H^* < 0$ and $J^* < 0$. The variation of the viscosity with temperature is described in Eq. (9), see [32, 47],

$$\frac{1}{\mu} = \frac{1}{\mu_\infty} [1 + A(T - T_w)] = B(T - T_r) \tag{9}$$

with

$$B = \frac{1}{\mu_\infty}, T_r = T_\infty - \frac{1}{A} \tag{10}$$

where A is a constant corresponding to the fluid thermal property, μ_∞ indicates the free stream fluid viscosity B and T_r are constants. In line with previous authors [48-49], similarity variables (11) are used to non-dimensional the modeled equations:

$$\begin{aligned} \eta &= y \sqrt{\frac{c(r+1)x^r}{2x\nu_\infty}}, \psi = x^{(r+1)/2} \sqrt{\frac{2c\nu_\infty}{(r+1)}} f(\eta), \omega = x^{(3r-1)/2} \sqrt{\frac{c^3(r+1)}{2\nu_\infty}} g(\eta), \\ u &= \frac{\partial \psi}{\partial y} = c x^r f', v = -\frac{\partial \psi}{\partial x} = -\sqrt{\frac{c\nu_\infty(r+1)}{2}} x^{(r-1)/2} \left(f + \frac{(r-1)}{(r+1)} \eta f' \right), \gamma = \left(\mu + \frac{\mu_r}{2} \right), \\ \theta(\eta) &= \frac{T - T_\infty}{T_w - T_\infty} = \frac{T - T_r}{T_w - T_\infty} + Q, Q = \frac{T_r - T_\infty}{T_w - T_\infty}, j = \left(\frac{\nu}{c} \right) x^{(1-r)} \end{aligned} \tag{11}$$

Furthermore, with the use of quantities in eq.(11) and taking cognizance of Eqs. (6-9) the governing Eqs. (2-4) yield the under listed equations:

$$\left(\frac{Q}{Q+\theta} + K \right) f''' + f f'' + K g' - \left(\frac{2}{r+1} \right) [(r+M) f'^2 - \lambda \theta \cos \varphi] + \frac{Q}{(Q-\theta)^2} \theta' f'' = 0, \tag{12}$$

$$\left(1 + \frac{K}{2} \right) g'' + f g' - \left(\frac{3r-1}{r+1} \right) f' g - \frac{2K}{r+1} (2g + f'') = 0, \tag{13}$$

$$\begin{aligned} (1 + Nr) \theta'' - \frac{2n}{(r+1)} \text{Pr} f \theta' + \text{Pr} \theta f' + \text{Pr} Ec \left(\frac{Q}{(Q+\theta)} + K \right) f''^2 + \frac{2n}{(r+1)} \text{PrMEc} f'^3 + \\ \frac{2n}{(r+1)} \text{Pr} (\alpha f' + \beta \theta) = 0, \end{aligned} \tag{14}$$

also, the boundary conditions become

$$\begin{aligned} f'(0) = 1, f(0) = f_w, g(0) = -hf'', \theta(0) = 1 \\ f'(\infty) = 0, g(\infty) = 0, \theta(\infty) = 0. \end{aligned} \tag{15}$$

where

$$\begin{aligned}
 fw &= -\sqrt{\frac{2\nu_0}{c\nu(r+1)}}, M = \frac{\sigma_0 B_0^2}{\rho_\infty}, \lambda = \frac{G_r}{\text{Re}^2}, Gr = g\beta_T \left(\frac{T_w - T_\infty}{\nu^2} \right) x^3, \text{Re} = \frac{u_w x}{\nu}, \\
 Nr &= -\frac{16\sigma^* T_\infty^3}{3k^* k}, Q = -\frac{1}{A(T_w - T_\infty)}, K = \frac{\mu_r}{\mu_\infty}, Ec = \frac{u_w^2}{c_p(T_w - T)}, \\
 Pr &= \frac{\mu_\infty c_p}{k}, \alpha = \frac{bk}{\mu_\infty c_p}, \beta = \frac{b^* k}{\mu_\infty c_p}.
 \end{aligned} \tag{16}$$

The parameters described in eq. (16) are defined in the nomenclature. The relevant quantities of engineering interest are the skin friction coefficient and the Nusselt number as given in eq. (17) in that order.

$$C_{f_x} = \frac{\tau_w}{\rho_\infty u_w^2}, Nu_x = \frac{xq_w}{k(T_w - T_\infty)} \tag{17}$$

with τ_w being shear stress and q_w heat flux at the surface such that

$$\tau_w = \left[(\mu + \mu_r) \frac{\partial u}{\partial y} + \mu_r \omega \right]_{y=0}, q_w = - \left[\left(k + \frac{16\sigma^* T_\infty^3}{3k^*} \right) \frac{\partial T}{\partial y} \right]_{y=0} \tag{18}$$

in view of Eqs. (11) and (18), the skin friction coefficient yields

$$C_{f_x} = \sqrt{\frac{r+1}{2}} \left(\frac{Q}{Q+\theta} + (1-h)K \right) (\sqrt{\text{Re}_x})^{-1} f''(0), \tag{19}$$

and the Nusselt number becomes

$$Nu_x = -\sqrt{\frac{\text{Re}_x(r+1)}{2}} (1 + Nr)\theta'(0) \tag{20}$$

3. Entropy Generation

In line with previous researchers (see [35, 40, 50]) the description of entropy generation rate in a radiative and dissipative hydromagnetic micropolar fluid flow of micropolar fluid can take the form

$$S_{gen} = \frac{k}{T^2} \left[(\nabla T)^2 + \frac{16\sigma^* T_\infty^3}{3k^* k} (\nabla T)^2 \right] + \frac{\mu + \mu_r}{T} \left(\frac{\partial u}{\partial y} \right)^2 + \frac{\sigma_0 (B(x))^2}{T} u^2 \tag{21}$$

The sources of entropy generation in eq. (21) include that of heat transfer which is indicated by the first term on the right of Eq. (21), the viscous dissipation induced entropy production as a result of fluid friction is denoted by the second term while the last term describes the generation of entropy by Ohmic heating. In dimensionless form, and setting $r = 1$, then Eq. (21) becomes:

$$Ns = \frac{S_{gen}}{S_{g_c}} = \frac{(1 + Nr)\theta'^2}{(\theta + \Omega)^2} + \frac{Br}{(\theta + \Omega)} \left(\frac{Q}{(Q + \theta)} + K \right) f''^2 + \frac{2BrM}{(\theta + \Omega)} \text{PrMEc} f'^3, \tag{22}$$

where Ns describes the overall entropy production in the system and $S_{g_c} = kc/\nu$ indicates the characteristic entropy generation. Moreso, $Br = Pr \times Ec$ denotes the Brikman number whereas $\Omega = T_\infty/(T_w - T_\infty)$ represents the non-dimensional temperature difference. It is quite essential to calculate the significant input of each source of entropy production in a system, in view of this, the Bejan number describes the proportion of the entropy production by heat transfer to the total proportion as represented in eq. (23) or (24).

$$\text{Be} = \frac{N_{ht}}{Ns} = \frac{N_{ht}}{N_{ht} + N_{vd} + N_{oh}} \tag{23}$$

or

$$\text{Be} = \frac{(1 + Nr)\theta'^2 (\theta + \Omega)^{-2}}{(1 + Nr)\theta'^2 (\theta + \Omega)^{-2} + (\theta + \Omega)^{-1} \left[Br \left(\frac{Q}{(Q + \theta)} + K \right) f''^2 + 2BrM f'^3 \right]}, \tag{24}$$

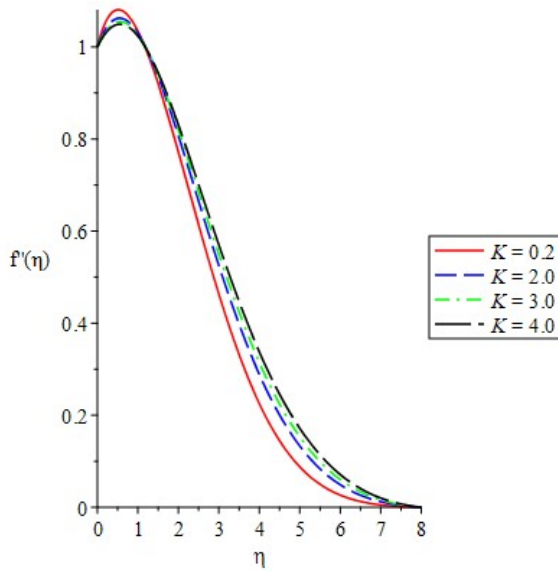


Fig. 2. Velocity field for micropolar parameter K

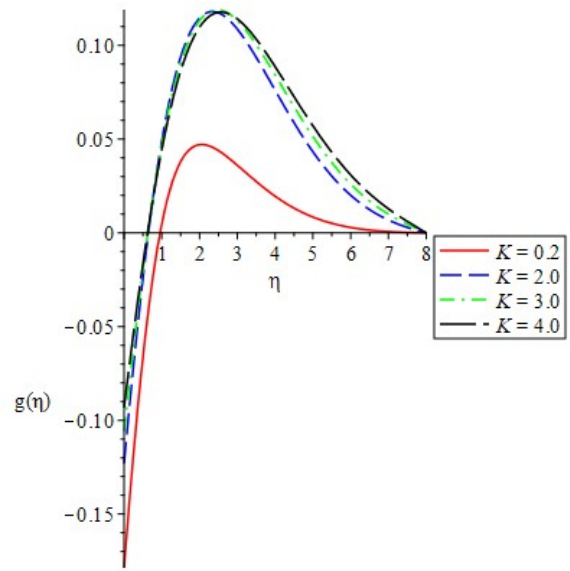


Fig. 3. Microrotation profiles for variation in K

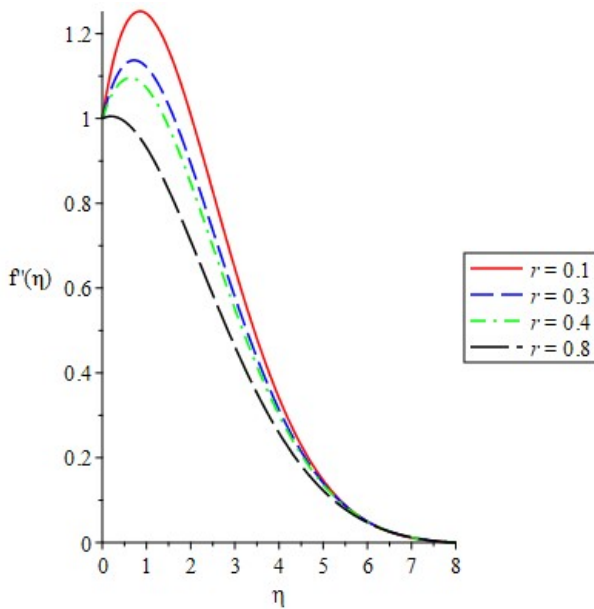


Fig. 4. Velocity field for variation of r

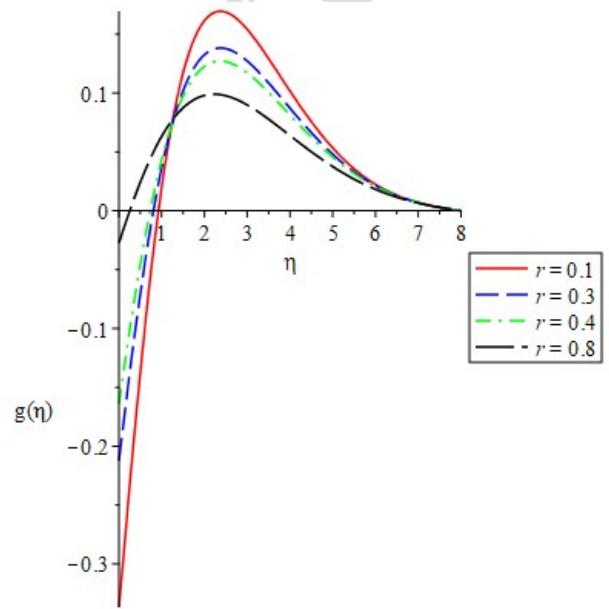


Fig. 5. The impact of r on microrotation profiles

where Be is the Bejan number N_{ht} , N_{vd} and N_{oh} represent entropy production from heat transfer, viscous dissipation, and Ohmic heating in that order. The Bejan number Be is given in Eq. (23 or 24) lies in the interval $0 \leq Be \leq 1$. The dominance of $(N_{vd} + N_{oh})$ over N_{ht} occurs when $Be = 0$ this indicates that entropy production as a result of heat transfer N_{ht} is dominated by those of viscous dissipation and Ohmic heating $(N_{vd} + N_{oh})$. Contrarily, when $Be = 1$ it implies that generation of entropy due to thermal heat transfer dominates that of viscous dissipation and Ohmic heating while the case $Be = 1/2$ signifies that $N_{ht} = (N_{vd} + N_{oh})$.

4. Numerical Method and its Validation

A computer algebra symbolic Maple 2016 package is used in solving Eqs. (12) to (14) together with the boundary conditions (15). The numerical procedure is based on Runge-Kutta techniques of fourth-order entrenched with a shooting scheme. To authenticate the numerical code employed in this study, the computational values of heat transfer at the sheet surface have been cross-checked with existing data reported by Grubka and Bobba [51] in the limiting condition that is recorded in Table 1. We hereby remarked that a good relationship exists between the current work and the existing work of [51]. Moreso, it is pointed out from Table 1 that higher values of Prandtl number enhance the transfer of heat. Similarly, an increase in the absolute value of the wall temperature parameter n facilitates the transfer of heat.

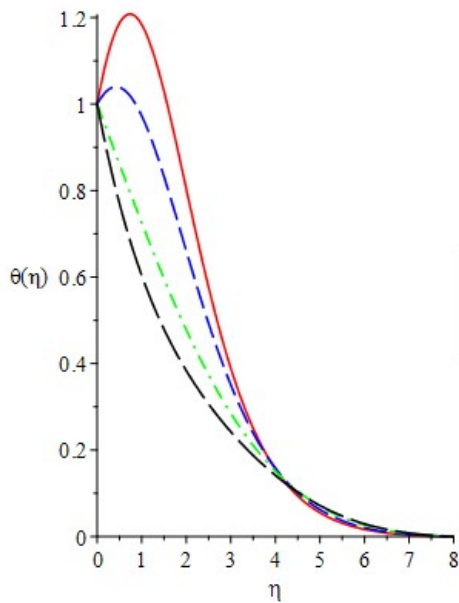


Fig. 6. The impact of n on temperature

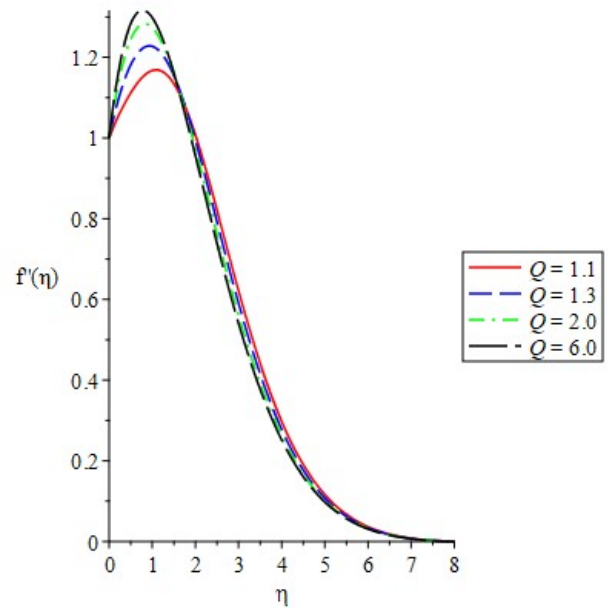


Fig. 7. The reaction of Q on velocity

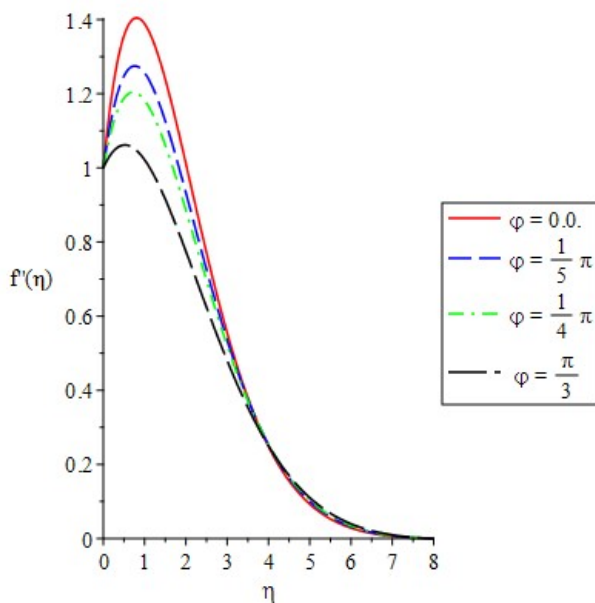


Fig. 8. The velocity field for varying φ

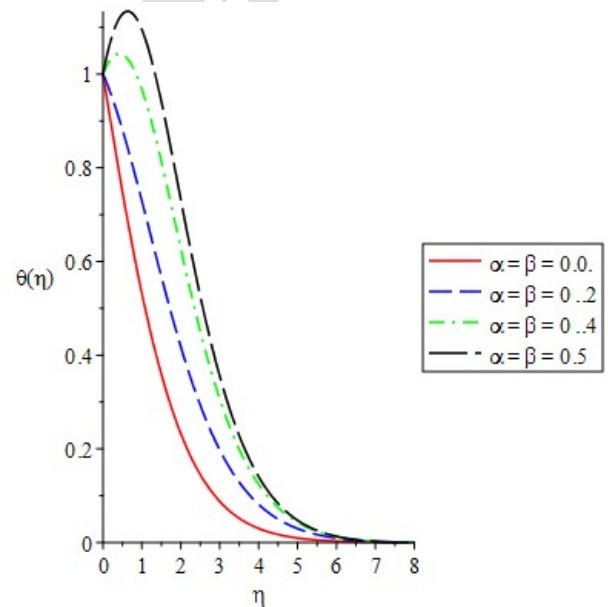


Fig. 9. Temperature profiles for changes in α / β

Table 1. Computed values of Nu_x as compared with [51] for changes in n and Pr , $r = 1, K = Ec = M = \alpha = \beta = fw = 0$ and $Q \rightarrow \infty$

n	Grubka & Bobba [51]		Present	
	$Pr = 0.72$	$Pr = 1.0$	$Pr = 0.72$	$Pr = 1.0$
- 2.0	0.7200	1.0000	0.72069	0.99945
- 1.0	0.0000	0.0000	-0.00110	0.00012
0.0	-0.4631	-0.5820	-0.46359	-0.58201
1.0	-0.8086	-1.0000	-0.80883	-1.00001
2.0	-1.0885	-1.3333	-1.08862	-1.33333
3.0	-1.3270	-1.6154	-1.32707	-1.61538

Likewise, the computed values C_{fx} are validated by those reported by Ulla *et al.* [52] as well as that of Lu *et al.* [53] for changes in the nonlinear stretching parameter r , these are displayed in Table 2. Observation reveals that with higher values of r , the skin friction coefficient C_{fx} advances which are in consonance with those authors compared with [56-57] as shown in Table 2.

Table 2. Computed values of C_{fx} as compared with existing results, variation of $r, K = Ec = \lambda = M = \alpha = \beta = fw = 0$ and $Q \rightarrow \infty$

r	Ulla <i>et al.</i> [52]	Lu <i>et al.</i> [53]	Present
0.0	0.6276	0.627547	0.627563
0.2	0.7668	0.766758	0.766846
0.5	0.8896	0.889477	0.889552
1.0	1.0000	1.000000	1.000008
1.5	-	1.061587	1.061609
3.0	1.1486	1.148588	1.148601
10.0	1.2349	-	1.234882
100.0	1.2768	-	1.276781

6. Results and Discussion

The reactions of the main physical parameters on the dimensionless velocity, microrotation, temperature, entropy generation rate and Bejan number are hereby presented in form of graphs with appropriate analysis. In the numerical computations carried out, use has been made of the following values as the default parameter values unless otherwise stated on the graphs. $Q = 5.0, K = M = 2.0, Ec = 0.1, \lambda = 4.0, r = n = Nr = 0.5, fw = 0.2 = Br = 0.2, \alpha = \beta = 0.3, Pr = 0.71, \varphi = \pi/6$ and $\Omega = 0.1$, Figures 2 and 3 exhibit the behavior of velocity and microrotation profiles with variation in the material (micropolar) parameter K .

The plot in Fig. 2 reveals that increasing the magnitude of K thickens the boundary layer and in consequence enhancing the velocity distribution. This response can be linked to a reduction in viscosity as the magnitude of material parameter K grows. In Fig. 3, it is noticeable that the microrotation profile appreciates from negative to positive as K rises in magnitude. The negative values illustrate that there is a reverse rotation of the micro-particles. The graph depicting the response of velocity profiles to variation in a nonlinear stretching parameter r is described in Fig. 4. One noticeable feature in this plot is that the hydrodynamic boundary layer thins out as r rises and in response, the fluid locomotion is reduced as seen in Fig. 4. This behavior is consistent with the report of [49]. On the other hand, the microrotation profiles fall with a rise in r with a reverse spinning of the micro-particles as demonstrated in Fig. 5. Figure 6 explains that the impact of the wall temperature parameter n is to reduce the thickness of the thermal boundary layer and consequently diminish the temperature distribution but enhances heat transfer. The behavior of the velocity field for changes in the viscosity parameter Q is demonstrated in Fig. 7. It is actually shown that the fluid velocity is lowered as the strength of the viscosity parameter Q grows, the stronger the viscosity, the lesser the fluid locomotion, this response agrees well with [19, 54]. Figure. 8 exhibits the behavior of velocity profiles with changes in the values of the inclination angle φ , it shows that increasing φ decelerates the fluid velocity. The velocity of the fluid when the sheet is vertical i.e. $\varphi = 0$ is shown to be higher than when the sheet is inclined, this is because the influence of buoyancy drops by a factor $\cos\varphi$ due to inclination and this leads to a reduction in the magnitude of the buoyancy driving force and at such less induced flow across the boundary layer takes place.

Meanwhile, the thermal boundary layer increases in thickness and the temperature field appreciates with a rise in both space and temperature-dependent heat source parameters α, β as displayed in Fig. 9. This observation agrees well with the physical point of view since the inclusion of α / β has the likelihood to boost the fluid temperature to rise.

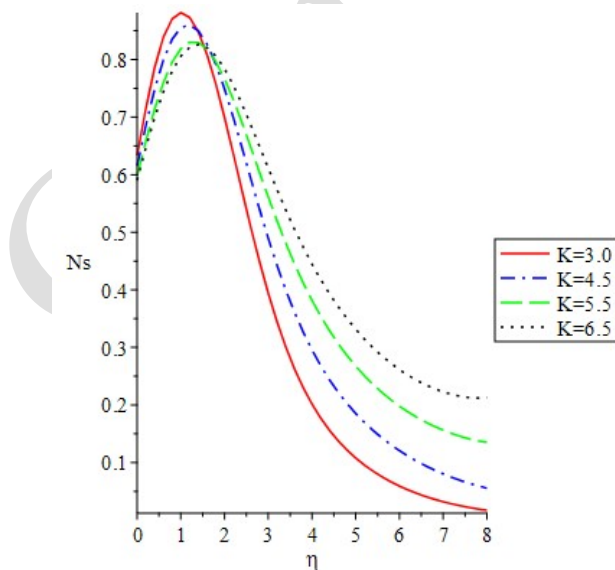


Fig. 10. Entropy generation for material parameter K

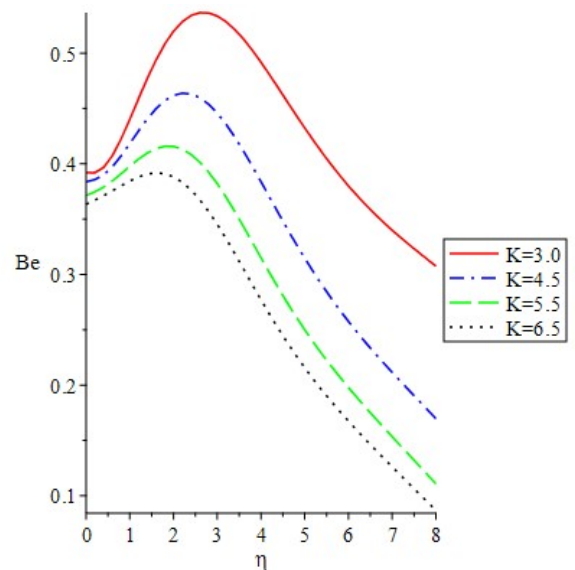


Fig. 11. Bejan number for K

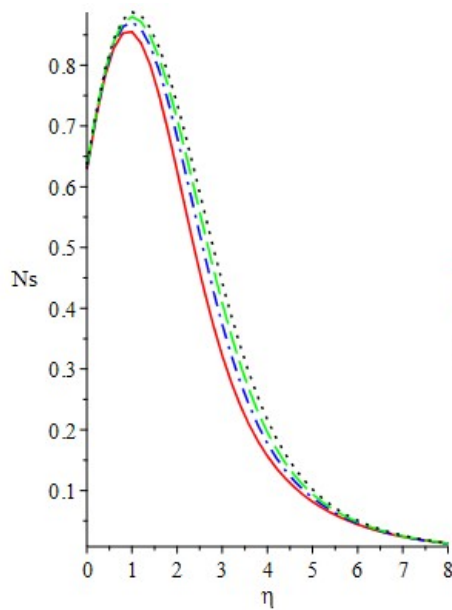


Fig. 12. Entropy generation for radiation parameter Nr

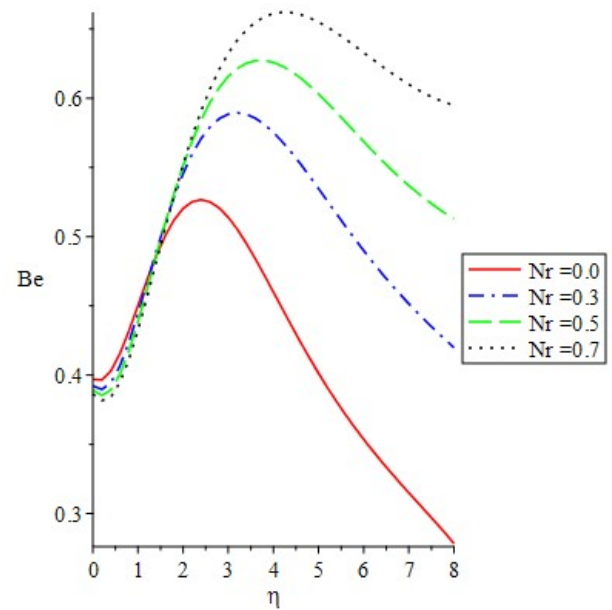


Fig. 13. Bejan number for radiation parameter Nr

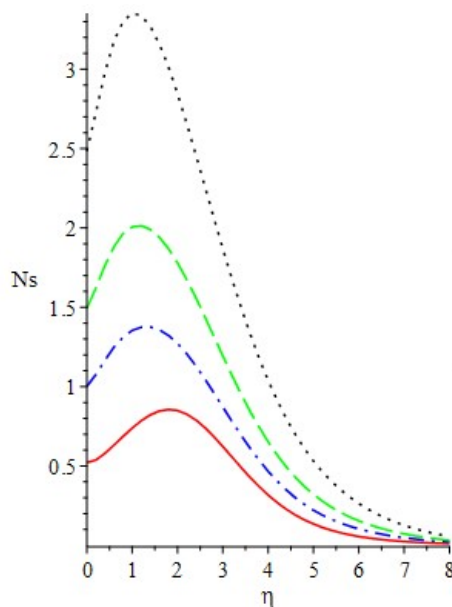


Fig. 14. Entropy generation for Brikman number Br

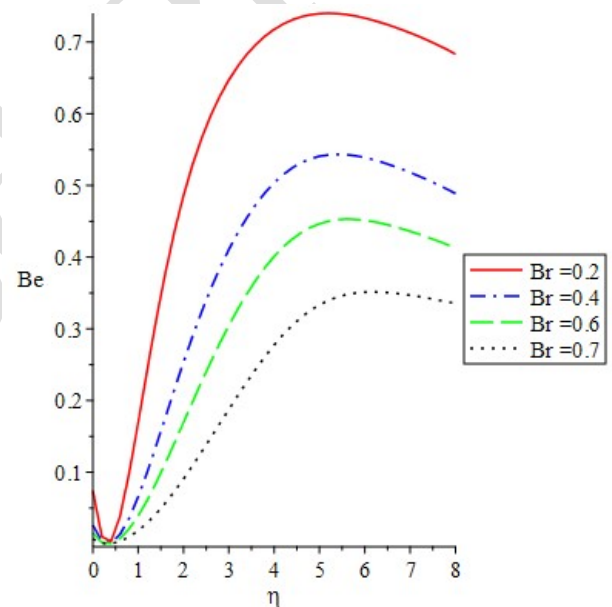


Fig. 15. Effect of Brikman number Br on Bejan number.

The graph showing the variation of K entropy generation rates Ns is demonstrated in Fig. 10. It conspicuously is shown that higher values of K decreases entropy generation close to the wall only but further away at a distance $\eta \approx 2.0$, the profiles intersect and a reverse trend is observed. However, Fig. 11 points out that the growth of K decelerates the Bejan number striking feature here is that heat transfer irreversibility falls with rising values of K while entropy production due to viscous dissipation and Ohmic heating take dominance.

The sketch relating to entropy generation versus η for variation in the radiation parameter Nr is displayed in Fig. 12.

It is revealed that a rise in Nr causes the entropy production in the system to rise, thus, the minimization of the entropy can be obtained by reducing the radiation. Figure 13 exhibits the response of Be with changes in the radiation parameter Nr , the fact from this plot indicates that with higher values of Nr , heat transfer irreversibility dominates that of viscous dissipation and Ohmic heating. Figure 14 behavior explains that rising values of Brikman number Br which is the product of Eckert and Prandtl number, causes the entropy production Ns to escalate especially near the sheet whereas with rising values of Br , the Bejan number Be falls as exhibited in Fig. 15 with the dominance of viscous and Ohmic heating irreversibility over heat transfer irreversibility.

7. Conclusion

Entropy generation in a hydromagnetic micropolar fluid passing an inclined nonlinear permeable stretching sheet with the impact of variable viscosity was analyzed in the current study. Solutions to the modeled equations were found by means of shooting techniques in the company with the Runge-Kutta algorithm. Validation of the numerical code was done with previously conducted related study in literature for some limiting conditions and found to be highly related. The influences of the main physical parameters were found and explained with the aid of different graphs. From our results, we note that:

- The entropy production advances with a rise in the radiation Nr and Brikman number Br whereas there is a fall in the entropy generation rate near the wall only with a rise in material(micropolar) parameter K .
- Heat transfer irreversibility takes preeminence over irreversibility due to viscous dissipation and Ohmic heating with an increase in the radiation parameter Nr whereas the opposite is the case with a rise in material (micropolar) K and Brikman number Br parameters.
- The velocity profiles appreciate for higher values of the material (micropolar) parameter K but the reverse trend occurs for the nonlinear stretching r and inclination angle parameters φ .
- The thermal boundary layer thickness grows with space and temperature-dependent heat source parameters α, β while the trend is reversed with a rise in wall temperature parameter n .

Author Contributions

In this work, author EOF formulated the problem, obtained the governing equations and transformed the governing equations from partial to ordinary differential equations. Subsequently, author SOS solved the governing equations and discuss the results obtained in this work. Both authors read and agreed on the issues discussed in the work.

Acknowledgments

The authors wish to acknowledge Professor S. S. Okoya of Obafemi Awolowo University, Ile-Ife, Nigeria and the anonymous reviewers for their useful suggestions and contributions in making this article a better one.

Conflict of Interest

The authors declare that there exists no conflict of interest as regards to the research work, authorship, and publication of this article.

Funding

The authors received no financial support for the research, authorship, and publication of this article.

Nomenclature

B_0	magnetic field strength [Wbm^{-2}]	u	velocity in x direction [$m s^{-1}$]
C_{fx}	skin friction coefficient	v	velocity in y direction [$m s^{-1}$]
c_p	specific heat capacity [J/kgK]	v_w	suction/injection velocity [$m s^{-1}$]
Ec	Eckert number	Greek Symbols	
f	non-dimensional stream function	α	space-dependent heat source/sink
fw	suction/injection parameter	β	temperature-dependent heat source/sink
g	non-dimensional microrotation	β_T	coefficient of thermal expansion [K^{-1}]
g_1	acceleration due to gravity	γ	spin gradient viscosity [$m^2 s^{-1}$]
j	micro inertial density [kgm^{-3}]	η	similarity variable
k	thermal conductivity [$Wm^{-1}K^{-1}$]	θ	dimensionless temperature
K	material parameter	λ	buoyancy parameter
k^*	mean absorption coefficient [m^{-1}]	μ_r	Vortex viscosity [$pa s$]
M	magnetic field parameter	μ	Newtonian viscosity [$kg m^{-1} s^{-1}$]
Nr	radiation parameter	ν	kinematic viscosity [$m^2 s^{-3}$]
Nu_x	Nusselt number	ρ	fluid density [$kg m^{-3}$]
Pr	Prandtl number	σ^*	Stefan-Boltzmannconstant [$Wm^{-1}K^4$]
Q	viscosity variation parameter	σ_0	electrical conductivity [$S m^{-1}$]

q'''	heat source [$Wm^{-3}K^{-1}$]	φ	inclination angle [rad]
q_w	surface heat flux [Wm^{-2}]	ψ	stream function [$m^2 s^{-1}$]
r	nonlinear stretching parameter	ω	microrotation component [s^{-1}]
T	temperature [K]	Superscripts and subscripts	
T_w	surface temperature [K]	w	surface conditions
T_∞	free stream temperature [K]	∞	free stream conditions


References

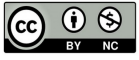
- [1] Srinivasacharya, D., Mendu, U., Free convection in MHD micropolar fluid with radiation and chemical reaction effects, *Chem. Ind. Chem. Eng.*, 20(2), 2014, 183-195.
- [2] Gaffar, S. A., Reddy, P. R., Prasad, V.R., Rao, A.S., Khan, B.Md., Viscoelastic micropolar convection flows from an inclined plane with nonlinear temperature: A numerical study, *J. Appl. Comput. Mech.*, 6(2), 2020, 183-199.
- [3] Eringen, A.C., Theory of micropolar fluids. *J. Math. Anal. Appl.*, 16, 1966, 1-18.
- [4] Eringen, A.C., Theory of thermo-micro fluids. *Journal of Mathematical Analysis and Applications*, 38, 1972, 480-496.
- [5] Lukaszewicz, G., *Micropolar fluids: Theory and Applications* (1st Ed.). Birkhauser, Boston, 1999.
- [6] Rahman, M.M., Convective flows of micropolar fluids from radiate isothermal porous surface with viscous dissipation and joule heating, *Commun Nonlinear Sci. Numer Simulat*, 14, 2009,3018-3030.
- [7] Reena, Rana, U.S., Effect of Dust Particles on rotating micropolar fluid heated from below saturating a porous medium, *Applications, and Applied Mathematics: An International Journal*, 4, 2009, 189-217.
- [8] Sakiadis, B.C., Boundary layer behavior on continuous solid surfaces: II The boundary layer on a continuous flat surface, *A.I.Ch.E.J.*, 7, 1961, 221-225.
- [9] Crane, L.J., Flow past a stretching plate, *Communications Breves*, 21, 1970, 645-647.
- [10] Gupta, P.S., Gupta, A.S., Heat and mass transfer on a stretching sheet with suction or blowing, *Can. J. Chem. Eng.*, 55, 1977, 744-746.
- [11] Vajravelu, K., Viscous flow over a nonlinearly stretching sheet, *Appl. Math. Comput.*, 124, 2001, 281-288.
- [12] Kumar, L., Finite element analysis of combined heat and mass transfer in hydromagnetic micropolar flow along a stretching sheet, *Comput Mater Sci*, 46, 2009, 841-848.
- [13] Renuka, P., Ganga, B., Kalaivanan, R., Hakeem, A.K., Slip effects on Ohmic dissipative non-Newtonian fluid flow in the presence of aligned magnetic field, *J. Appl. Comput. Mech.*, 6(2), 2020, 296-306.
- [14] Qasim, M., Khan, I., Shafie, S. Heat transfer in a micropolar fluid over a stretching sheet with Newtonian heating, *Plos One*, 8(4), 2013, 1-6.
- [15] Cortell, R., Viscous flow and heat transfer over a nonlinearly stretching sheet, *Applied Mathematics and Computation*, 184, 2007, 864-873.
- [16] Cortell, R., Effects of viscous dissipation and radiation on the thermal boundary layer over a nonlinearly stretching sheet, *Physics Letters A*, 372, 2008, 631-636.
- [17] Alinejad, J., Samarbakhsh, S., Viscous flow over nonlinearly stretching sheet with effects of viscous dissipation, *Journal of Applied Mathematics*, 2012, 2012, 1-10.
- [18] Daniel, Y.S., Steady MHD boundary layer slip flow and heat transfer of nanofluid over a convectively heated of a nonlinear permeable sheet, *Journal of Advanced Mechanical Engineering*, 3, 2015, 1-14.
- [19] Salem, A.M., The effects of variable viscosity, viscous dissipation and chemical reaction and heat and mass transfer of flow of MHD micropolar fluid along a permeable stretching sheet in a non-darcian porous medium, *Mathematical Problems in Engineering*, 2013,1-10.
- [20] Hsiao, K.L., Heat and mass transfer for micropolar flow with radiation effect past a nonlinearly stretching sheet, *Heat Mass Transfer*, 46, 2010, 413-419.
- [21] Ahmad, K, Ishak, A., Nazar, R., Micropolar fluid flow and heat transfer over a nonlinearly stretching plate with viscous dissipation, *Mathematical Problems in Engineering*, 2013, 1-5.
- [22] Kumar, B., Srinivas, S., Unsteady hydromagnetic flow of Eyring-Powell Nanofluid over an inclined permeable stretching sheet with joule heating and thermal radiation, *J. Appl. Comput. Mech.*, 6(2), 2020, 259-270.
- [23] Waqas, M., Farooq, M., Khan, M.J., Alsaedi, A., Hayat, T., Yasmeen, T., Magnetohydrodynamic (MHD) mixed convection flow of micropolar liquid due to nonlinear stretched sheet with convective condition, *International Journal of Heat and Mass Transfer*, 102, 2016, 766-772.
- [24] Shamshuddin, M.D., Thumma, T., Numerical study of dissipative micropolar fluid flow past an inclined porous plate with heat source/sink, *Propulsion and Power Research*, 8(1), 2017, 56-68.
- [25] Khan, W., Gul, T., Idrees, M., Islam, S, Khan, I., Dennis, L. C.C., Thin-film Williamson nanofluid flow with varying viscosity and thermal conductivity on a time-dependent stretching sheet, *Applied Sciences*, 6, 2016,1-33.
- [26] Rahman, M. M., Locally similar solutions for hydromagnetic and thermal slip flow boundary layers over a flat plate with variable fluid properties and convective surface boundary condition, *Meccanica*, 46, 2011,1127-1143.
- [27] Akinbobola, T. E., Okoya, S. S., The flow of second-grade fluid over a stretching sheet with variable thermal conductivity and viscosity in the presence of heat source/sink, *Journal of Nigeria Mathematical Society*, 34, 2015, 331-342.

- [28] Fatunmbi, E. O., Fenuga, O. J., MHD micropolar fluid flow over a permeable stretching sheet in the presence of variable viscosity and thermal conductivity with Soret and Dufour effects, *International Journal of Mathematical Analysis and Optimization: Theory and Applications*, 2017, 211- 232.
- [29] Kobo, N.S., Makinde, O.D., Second law analysis for variable viscosity reactive Couette flow under Arrhenius kinetics, *Mathematical Problems in Engineering*, 2010, 1-15
- [30] Bejan, A., Second law analysis in heat transfer and thermal design, *Adv. Heat Transf.*, 15, 1982, 1-58.
- [31] Bejan, A., *Entropy Generation Minimization*, CRC: Boca Raton, FL, USA. 1996.
- [32] Makinde, O.D., Second law analysis for variable viscosity hydromagnetic boundary layer flow with thermal radiation and Newtonian heating, *Entropy*, 13(8), 2011, 1446-1464.
- [33] Salawu, S.O., Kareem, R A., Shonola, S. A. Radiative thermal criticality and entropy generation of hydromagnetic reactive Powell-Eyring fluid in saturated porous media with variable conductivity, *Energy Reports*, 5, 2019, 480-488.
- [34] Alsabery, A.I., Ishak, M.S., Chamkha, J. A., Hashim, I. Entropy Generation Analysis and Natural Convection in a Nanofluid-Filled Square Cavity with a Concentric solid insert and different temperature distributions, *Entropy*, 20, 2018, 1-24.
- [35] Afridi, M.I., Qasim, M., Khan, I., Shafie, S., Alshomran, A.S., Entropy generation in magnetohydrodynamic mixed convection flow over an inclined stretching sheet, *Entropy*, 19, 2017, 1-11.
- [36] Eegunjobi, A. S., Makinde, O.D., Irreversibility analysis of MHD Buoyancy-driven variable viscosity liquid film along an inclined heated plate convective cooling, *Journal of Applied and Computational Mechanics*, 5(5), 2019, 840-848.
- [37] Salawu, S.O., Fatunmbi, E.O. Inherent irreversibility of hydromagnetic Third-grade reactive Poiseuille flow of a variable viscosity in porous media with convective cooling, *Journal of the Serbian Society for Computational Mechanics*, 11(1), 2017, 46-58.
- [38] Afridi, M.I., Qasim, M., Makinde, O.D. Minimization of entropy production in three-dimensional Dissipative flow of Nanofluid with graphene nanoparticles: A numerical study, *Defect and Diffusion Forum*, 387, 2018, 157-165.
- [39] Ishak, M., Ali, G., Sha, Z., Islam, S., Muhammad, S., Entropy generation on nanofluid thin film of Eyring-Powell fluid with thermal radiation and MHD effect on an unsteady porous stretching sheet, *Entropy*, 20, 2018, 1-24.
- [40] Afridi, M.I., Qasim, M., Makinde, O.D. Entropy generation due to heat and mass transfer in a flow of dissipative elastic fluid through a porous medium, *Journal of Heat Transfer*, 141, 2019, 1-9.
- [41] Rahman, M.M., Aziz, A., Al-Lawatia, M.A., Heat transfer in micropolar fluid along an inclined permeable plate with variable fluid properties, *International Journal of Thermal Sciences*, 49, 2010, 993-1002.
- [42] Das, K., Slip effects on heat and mass transfer in MHD micropolar fluid flow over an inclined plate with thermal radiation and chemical reaction, *Int. J. Numer. Meth. Fluids*, 70(1), 2012, 96-113.
- [43] Ishak, A., Similarity solutions for flow and heat transfer over a permeable surface with convective boundary condition, *Applied Mathematics, and Computation*, 217, 2010, 837-842.
- [44] Yazdi, M.H., Abdullah, S., Hashim, I. and Sopian, K. Effects of viscous dissipation on the slip MHD flow and heat transfer past a permeable surface with convective boundary conditions, *Energies*, 4, 2011, 2273-2294.
- [45] Helmy, K.A., MHD boundary layer equations for power-law fluids with variable electric conductivity, *Meccanica*, 30, 1995, 187-200.
- [46] Pal, D., Mondal, H., Effect of Soret Dufour, chemical reaction and thermal radiation on MHD non-Darcy unsteady mixed convective heat and mass transfer over a stretching sheet, *Commun. Nonlinear Sci. Numer. Simulat.*, 16, 2011, 1942-1958.
- [47] Ling, J., Dybbs, A., Forced convection over a flat plate submerged in a porous medium: variable viscosity case, *American Society of Mechanical Engineers*, 1987, 13-18.
- [48] Rawat, S., Kapoor, S., Bhargava, R., MHD flow heat and mass transfer of micropolar fluid over a nonlinearly stretching sheet with variable micro inertial density, heat flux and chemical reaction in a non-Darcy medium, *Journal of Applied Fluid Mechanics*, 9(1), 2016, 321-331.
- [49] Hayat, T., Abbas, Z., Javed, T., Mixed convection flow of a micropolar fluid over a non-linearly stretching sheet, *Physic Letter A*, 372, 2008, 637-647.
- [50] El-Aziz, M, Saleem, S., Numerical simulation of entropy generation for power-law liquid flow over a permeable exponential stretched surface with variable heat source and heat flux, *Entropy*, 21, 2019, 1-19.
- [51] Grubka, L.J., Bobba, K.M., Heat transfer characteristic of a continuous stretching surface with variable temperature, *Journal of Heat Transfer*, 107, 1985, 248-250.
- [52] Ullah, I., Shafie, S., Khan, I., Effects of slip condition and Newtonian heating on MHD flow of Casson fluid over a nonlinearly stretching sheet saturated in a porous medium, *Journal of King Saud University Science*, 29, 2017, 250-259.
- [53] Lu, D., Ramzan, M., Ahmadi, S. Chung, J. D., Farooq, U., A numerical treatment of MHD radiative flow of micropolar nanofluid with homogeneous-heterogeneous reactions past a nonlinear stretched surface, *Scientific Reports*, 8, 2018, 1-17.
- [54] Seddeek, M. A., Salem, A.M. Further results on the variable viscosity with magnetic field on flow and heat transfer to a continuous moving flat plate, *Physics Letters A*, 353, 2006, 337-340.

ORCID iD

E.O. Fatunmbi  <https://orcid.org/0000-0001-8656-6520>

S.O. Salawu  <https://orcid.org/0000-0001-6951-7524>



© 2020 by the authors. Licensee SCU, Ahvaz, Iran. This article is an open access article distributed under the terms and conditions of the Creative Commons Attribution-NonCommercial 4.0 International (CC BY-NC 4.0 license) (<http://creativecommons.org/licenses/by-nc/4.0/>).

How to cite this article: Fatunmbi, E.O., Salawu, S.O. Analysis of Entropy Generation in Hydromagnetic Micropolar Fluid Flow over an Inclined Nonlinear Permeable Stretching Sheet with Variable Viscosity, *J. Appl. Comput. Mech.*, 7(1), 2021, x-xx. <https://doi.org/10.22055/JACM.2019.30990.1807>

Corrected Proof